Tailoring of the Perpendicular Magnetization Component in Ferromagnetic Films on a Vicinal Substrate

A. Stupakiewicz,[1] A. Maziewski,[1] K. Matlak,[2] N. Spiridis,[3] M. Ślęzak,[2] T. Ślęzak,[2] M. Zając,[2] and J. Korecki[2,3]

[1]*Laboratory of Magnetism, University of Bialystok, Lipowa 41, 15-424 Bialystok, Poland*

[2]*Faculty of Physics and Applied Computer Science, AGH-University of Science and Technology, 30-059 Krakow, Poland*

[3]*Institute of Catalysis and Surface Chemistry, Polish Academy of Sciences, 30-239 Krakow, Poland*

(Received 20 March 2008; published 20 November 2008)

We have engineered the magnetic properties of 1–8 nm Co films epitaxially grown on an Au-buffered bifacial W(110)/W(540) single crystal. The surface of Au/W(110) was atomically flat, whereas the Au/W(540) followed the morphology of the vicinal W surface, showing a regular array of monoatomic steps. For Co grown on Au/W(540), the existence of the out-of-plane magnetization component extended strongly to a thickness d of about 8 nm, which was accompanied by an anomalous increase of the out-of-plane switching field with increasing d. In addition, the process of up-down magnetization switching could be realized with both a perpendicular and in-plane external magnetic field.

DOI: 10.1103/PhysRevLett.101.217202 PACS numbers: 75.70.−i, 75.30.Gw, 78.20.Ls

Perpendicular magnetization, essential for applications in high density magnetic storage media, is an important feature of low dimensional magnetic systems. Typically, such a magnetic configuration in a ferromagnetic ultrathin film results from a competing magnetocrystalline volume and surface or interface anisotropies, and involves a spin reorientation transition (SRT) from an in-plane to a perpendicular magnetization direction with decreasing film thickness, as was observed for the first time by Gradmann and Müller [1]. Among many thin film epitaxial systems in which a perpendicular magnetization and SRT were found (for review, see [2]), for cobalt on Pt and Au, the perpendicular magnetization persists up to relatively large values of the Co film thickness. It is known that the critical SRT thickness for ultrathin Au/Co/Au(111) is slightly below 2 nm [3,4]. Remarkably, SRT strongly depends on the substrate morphology, which can be modified in a controlled way by using vicinal surfaces (which provide a regular array of oriented atomic steps with a precisely determined density). The stepped substrates are often used as templates for the growth of magnetic self-organized nanostructures, such as atomic wires [5] or ultrathin stripes [6] and also for tailoring magnetic structure, since the step contribution to the magnetic anisotropy of the spin-orbit interaction can be comparable to the surface interaction [7–10]. The critical thickness of SRT for Co films on Au(788) is less than on the flat Au(111) substrate [11]. The dipolar interaction always favors magnetization along steps, while the Néel-type step anisotropy, depending on the system, can prefer magnetic directions parallel or perpendicular to the steps [2,12]. Additionally, Kawakami *et al.* [13] observed a slight (15%) shift of the SRT thickness for Fe on stepped Ag(001).

In our report, epitaxial Co films deposited on a reference, an atomically flat Au/W(110), and a vicinal Au/W(540) substrate were studied. We found that, for Co deposited on the vicinal substrate, an out-of-plane magnetization state could be observed for cobalt films as thick as $d = 8$ nm. The process of up-down magnetization switching could be induced by both perpendicular and in-plane external magnetic fields. These results suggest a new class of magnetic recording media that have out-of-plane magnetic moments but are switchable with in-plane magnetic fields. In addition, an anomalous increase of the perpendicular switching field with increasing d was observed for Co deposited on the stepped Au surface. The samples were prepared and characterized in an ultra high vacuum (UHV) system. A bifacial W single crystal [see Fig. 1(a)] assembling both surfaces (flat W(110) and vicinal W(540) with a 6.34° miscut angle relative to the W[1–10] direction of the W(110) surface) was cleaned by repeated heating to 1500 K at an oxygen pressure of 10^{-7} mbar followed by flashing to above 2100 K. The atomic scale purity of the tungsten surfaces was verified by Auger electron spectroscopy. The structure and magnetic properties of the samples were monitored *in situ* by low energy electron diffraction (LEED) and the magneto-optical Kerr effect (MOKE). The typical (1×1) LEED pattern could be observed on the W(110) substrate part, whereas the W(540) surface gave split diffraction spots, indicating the presence of ordered monatomic steps parallel to the W[001] direction [Fig. 1(b)]. The average terrace width for the W(540) surface could be estimated as 2 nm, in perfect agreement with the nominal value 2.014 nm. The sample configuration is schematically shown in Fig. 1(a). A 5 nm thick Au buffer layer was deposited on both tungsten surfaces at room temperature. From the symmetry of the LEED pattern, it can be concluded that a slightly distorted Au(111) grows on W(110), with the Au[−211] direction parallel or close to the W[1–10] direction, in rough agreement with previous studies [14]. The vicinality of the Au surface on W(540) is clear from the LEED

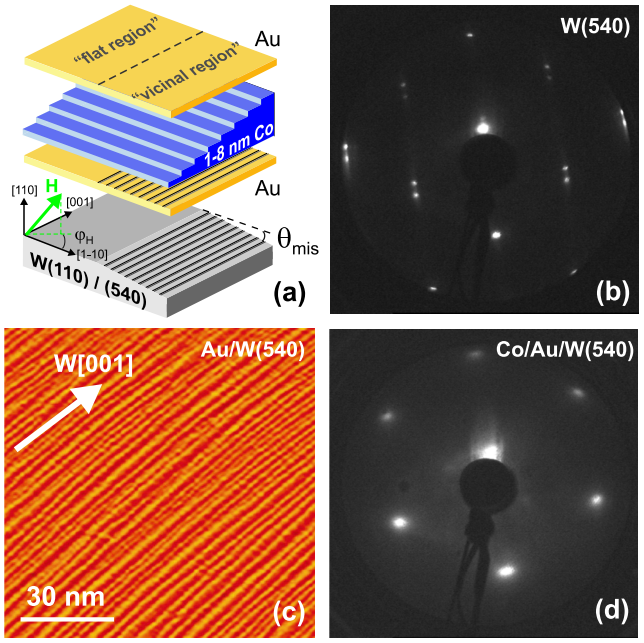

FIG. 1 (color online). Schematic configuration of the sample (a). LEED patterns on the vicinal surface at different preparation stages: (b) W(540) surface, (d) 8 nm Co film surface, and (c) STM images for 5 nm Au on W(540). LEED patterns were taken at electron energy of 120 eV.

patterns, and the analysis of the spot splittings points to the Au(544) surface. Such a surface (nominal miscut 6.21° towards the [2-1-1] azimuths with respect to the [111] direction) consists of nine-atomic rows of Au(111) terraces, separated by monoatomic steps along the dense packed [0–11] directions. The stepped morphology of the Au surface was confirmed also by scanning tunneling microscopy (STM) measurements, performed in another UHV system, as can be seen from the image in Fig. 1(c). On the Au buffer layer, using a movable shutter, a striped Co layer, with an individual stripe thickness d ranging from 1 to 8 nm, was simultaneously grown at room temperature on both flat and vicinal parts of the substrate [see Fig. 1(a)]. Cobalt grows epitaxially on Au(111) and Au (544), and homogenously broadened LEED spots indicated a grainy Co structure, also confirmed by STM, with a typical grain size of several nanometers. Characteristically, the step structure is not transferred to the Co surface, for which LEED reveals (1×1) patterns relative to the Au (111) surface [Fig. 1(d)]. This also holds for the final 2 nm thick Au protective layer, which enables *ex situ* studies.

The magnetization reversal process and magnetic anisotropy were studied in detail *ex situ* at room temperature using a MOKE-based magnetometer with $\lambda = 640$ nm laser light. The perpendicular magnetization component was measured using polar MOKE (*P*-MOKE) geometry, with the angle of incidence of the laser light close to the sample normal and the external magnetic field $H_\perp$ perpendicular to the crystal surface. For the purpose of the vector magnetometry [15], an additional in-plane magnetic field could be applied. The perpendicular magnetization component could also be derived from the longitudinal MOKE (*L*-MOKE) data, after separation of the polar component. The measurements of the longitudinal hysteresis loops were performed with the in-plane external magnetic field $H_\parallel$ applied along various angles φ_H with respect to the W [1–10] direction [see Fig. 1(a)].

The rectangular shape of *P*-MOKE hysteresis loops observed for the 1 nm thick Co film grown on both the flat and vicinal substrate parts indicates a perpendicular magnetization of Co (see Fig. 2). For the Co film on the flat Au, the shape of the polar magnetization curves changed with increasing Co thickness, showing a gradual reduction of the remanent magnetization (normalized to the saturation magnetization $M_r = (M_{(H=0)}/M_s)$ and coercive field, accompanied by an increase of the saturation field. Above a certain critical thickness, the *P*-MOKE magnetization curve with zero remanence was observed; this is exemplified by the sample of Co with a thickness of 3 nm by open points in Fig. 2, indicating the reorientation of the easy magnetization direction from the out-of-plane to an in-plane orientation. The critical thickness of this SRT for the flat region, estimated from the *P*-MOKE and *L*-MOKE data to be close to $d = 2$ nm, is slightly higher than the literature data for typical Au/Co/Au films on flat substrates [3,4]. A different situation was found for the Co layer grown on the vicinal substrate where, over the entire investigated Co thickness range, the out-of-plane magnetization component was observed in the MOKE measurements. This can be clearly seen by comparison of the small

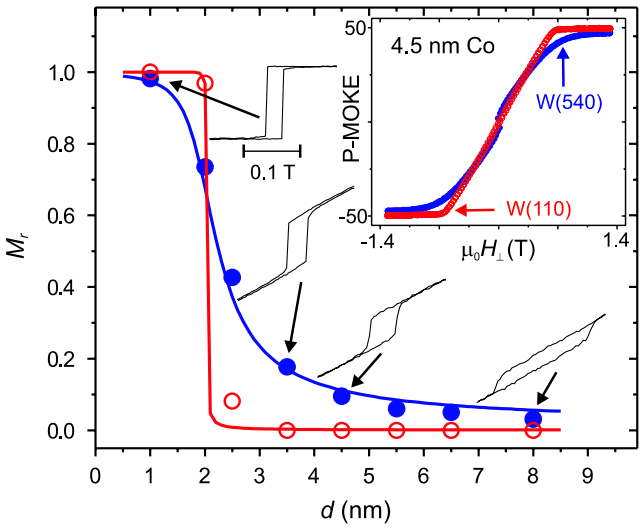

FIG. 2 (color online). Dependence of normalized remanent magnetization M_r on the Co thickness for W(110) (open points) and W(540) (full points) substrate regions. Solid lines are calculated within the proposed model (Eq. (1)). Inset: the hysteresis loops for the 4.5 nm thick Co film on both the flat and vicinal region measured by *P*-MOKE. The loops linked with the arrows to the full points show a small field range for 1, 3.5, 4.5 and 8 nm thick Co on the vicinal surface.

field P-MOKE hysteresis curves recorded for different Co thickness, as well as from the loop measured at $d = 4.5$ nm, shown in Fig. 2 and its inset, respectively. The shape of the P-MOKE hysteresis loop indicates that the magnetization reversal process induced by the $H_\perp$ field occurs by switching the normal magnetization component followed by coherent magnetization rotation. The thickness dependence of the remanent magnetization obtained from the normalized P-MOKE loops is plotted in Fig. 2 for the Co films grown on the both substrates. For the Co/Au/W(540) system, both a shift of the SRT and a change of the transition character can be deduced. It is also clear that the canting angle of the magnetization can be controlled with the Co thickness. On the contrary, for Co grown on the flat substrate, a different mechanism of SRT is manifested by a sharp $M_r(d)$ profile.

The in-plane magnetization curves measured with the external magnetic field $H_\parallel$ along the [1–10] and [001] directions for the 4.5 nm thick Co film on the flat and vicinal substrate are shown in Fig. 3(a) and 3(b), respectively. The shape of the loops indicates that the easy in-plane magnetization axis is parallel to the W[1–10] direction, i.e., to Au[−211] in the both substrate regions. The angular dependence of the coercive field determined from the L-MOKE loops that is registered for the various angles φ_H is also shown in Fig. 3(c). The twofold symmetry of the in-plane magnetic anisotropy can be concluded for Co deposited on the flat Au(111)/W(110) substrate, reflecting the symmetry of the misfit strains in the Co/Au/W system. The magnetization reversal induced by $H_\parallel$ occurs in the plane of the sample without a change of the perpendicular magnetization component, as can be seen from the isotropic character of the polar component measured in $H_\parallel = 0.14$ T, shown in Fig. 3(e). Similarly, the twofold symmetry of the in-plane angular dependence of the coercive field was observed also for Co on the vicinal surface, see Fig. 3(d). Contrary to the process in the perpendicular magnetic field, the vectorial magnetometry showed that the magnetization reversal process induced by $H_\parallel$ occurs in the three dimensional space, involving a change of the perpendicular magnetization component. This can be seen from the polar plot in Fig. 3(f), presenting the azimuthal dependence of the polar components for the in-plane magnetization reversal. The switching of the perpendicular magnetization component could be also directly seen from the polar hysteresis loop (with the laser light along the surface normal) with the in-plane external field $H_\parallel$, as shown in the upper inset to Fig. 4.

For the quantitative analysis of the MOKE measurements, the following expression for Co film anisotropy energy was assumed:

$$E_A(\theta, \varphi) = K_{u1}[1 - (\mathbf{m} \cdot \mathbf{v}_{\mathrm{mis}})^2] - \tfrac{1}{2}\mu_0 M_s^2 \sin^2\theta + K_{u2}[1 - (\mathbf{m} \cdot \mathbf{v}_{\mathrm{mis}})^2]^2 + K_{\mathrm{in}} \sin^2\theta \sin^2\varphi, \quad (1)$$

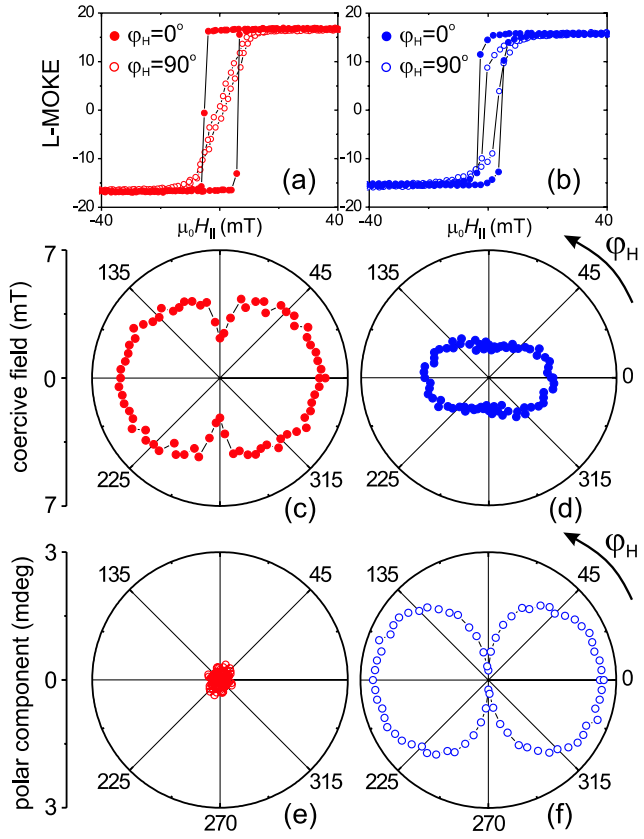

FIG. 3 (color online). Hysteresis loops measured as longitudinal Kerr ellipticity for the in-plane magnetic field applied along W[1–10] and W[001] directions for a Co thickness $d = 4.5$ nm (a),(b). Also, polar plots of the angular dependence of the coercive field (c),(d) and the polar component measured at $H_\parallel = 0.14$ T for the in-plane field magnetization reversal (e),(f) are shown (left column) flat W(110) and (right column) W(540) region.

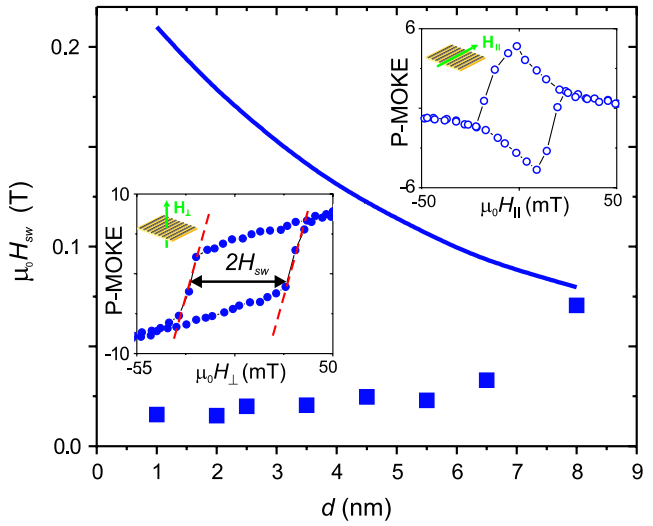

FIG. 4 (color online). Thickness dependence of H_{sw} for Co on the vicinal substrate. The solid line represents the $H_{\mathrm{sw}}^{\mathrm{max}}$ field calculated using Eq. (2). The insets show the P-MOKE loops for a Co thickness of 4.5 nm measured as a function of the perpendicular (lower curve) and in-plane (upper curve) magnetic field.

where **m** is the normalized magnetization vector defined by polar and azimuthal angles θ and φ, respectively, (φ is measured from the W[1–10] direction), $\mathbf{v_{mis}}$ is the unit vector defining the miscut direction, $\mathbf{v_{mis}} = (\sin\theta_{\mathrm{mis}}, 0, \cos\theta_{\mathrm{mis}})$, and K_{in} is the in-plane anisotropy constant. The classical thickness dependence of the out-of-plane anisotropy constant, $K_{u1}(d) = K_v + 2K_s/d$, is assumed taking into account the volume K_v and surface K_s anisotropy constants. The miscut unit vector was taken to be $\mathbf{v_{mis}} = (0, 0, 1)$ for the flat region. The bulk value of saturation magnetization ($M_s = 1400$ A/m) was assumed for the whole Co thickness range. First, for Co deposited on the flat substrate, the effective anisotropy constants were determined from the hard axis *P*-MOKE hysteresis loops dominated by the coherent magnetization rotation for $d > 2$ nm. The volume $K_v = 0.29$ MJ/m^3 and the surface $K_s = 1.16$ mJ/m^2 anisotropy contributions were determined from the fitted hysteresis loops for different Co thicknesses. The basic influence of the steps on the perpendicular magnetization component is reflected in two constants of uniaxial out-of-plane and in-plane anisotropy. It is important to note that the K_{in} constant is approximately an order of magnitude smaller than the perpendicular one (K_{u1}) [16]. The magnetic anisotropy constants K_v and K_s determined for the Co films grown on the flat reference region, were used for the fitting the *P*-MOKE loops measured for Co on the vicinal part. The thickness dependence of the normalized perpendicular remanent magnetization $M_r(d)$ Fig. 2 calculated using Eq. (1) (assuming $\theta_{\mathrm{mis}} = 6.34°$ for vicinal and 0.1° for flat substrates) agrees very well with the experimental points.

The perpendicular switching field H_{sw} for Co on the vicinal substrate, derived from the *P*-MOKE data, is shown in Fig. 4. The switching is observed in the whole range of Co thicknesses. The theoretical value of the switching field, H_{sw}, for the given Co thickness could be obtained from the minimization of the sum of the anisotropy energy E_A and the Zeeman energy in the perpendicular external magnetic field. With increasing $H_\perp$, the magnetization rotates towards the sample plane and approaches $\theta = 90°$ for

$$H_{\mathrm{sw}}^{\mathrm{max}} = \frac{K_{u1}\sin 2\theta_{\mathrm{mis}} + 4K_{u2}\sin^3\theta_{\mathrm{mis}}\cos\theta_{\mathrm{mis}}}{\mu_0 M_s}, \quad (2)$$

where $H_{\mathrm{sw}}^{\mathrm{max}}$ is the upper limit of the switching field H_{sw} (defined in the inset in Fig. 4) for the vicinal surface. The calculated $H_{\mathrm{sw}}^{\mathrm{max}}(d)$ dependence is shown by the continuous line in Fig. 4. For a small Co thickness, the magnetic reversal process occurs in a magnetic field much smaller than $H_{\mathrm{sw}}^{\mathrm{max}}$. The process is connected with nucleation of reversed domains and propagation described by the coercive field [17]. With increasing d, magnetization rotation towards the direction of the applied field becomes more important and the switching field approaches $H_{\mathrm{sw}}^{\mathrm{max}}$. It can be clearly seen in Fig. 4 that the experimental H_{sw} approaches the theoretically determined $H_{\mathrm{sw}}^{\mathrm{max}}$ for $d = 8$ nm.

In conclusion, we have studied the magnetic properties Au/Co/Au films deposited on both a flat W(110) and vicinal W(540) substrate. On W(540), we observed the out-of-plane magnetization state in the whole Co thicknesses range, from 1 to 8 nm, with an easy magnetization axis that increases in inclination from the normal with an increase of the Co thickness. The magnetization could be switched between the two magnetic states by both a perpendicular and in-plane magnetic field, and the perpendicular switching field increased with increasing Co thickness. We proposed a phenomenological, simplified model that describes the magnetic properties of the Co films on the vicinal surface well, involving only magnetic parameters of the film on the flat substrate and the geometrical factor of vicinality. As was shown recently, self-organized nanostructures grown on vicinal substrates provide a unique opportunity to engineer the spin-orbit interaction [5]. The present results can be applied for a broad class of magnetic thin films, thus allowing one to control the perpendicular magnetic anisotropy and out-of-plane magnetization states of a material, which is interesting for basic knowledge and possible applications.

This work was supported in part by the Marie Curie Grants for "Transfer of Knowledge" NANOMAG-LAB (No. 2004-003177) and Polish Scientific Network ARTMAG.

[1] U. Gradmann and J. Müller, Phys. Status Solidi **27**, 313 (1968).
[2] P. J. Jensen and K. H. Bennemann, Surf. Sci. Rep. **61**, 129 (2006).
[3] *Ultrathin Magnetic Structures*, edited by J. Bland and B. Heinrich (Springer, Berlin, 1994).
[4] M. Kisielewski, A. Maziewski, M. Tekielak, A. Wawro, and L. T. Baczewski, Phys. Rev. Lett. **89**, 087203 (2002).
[5] P. Gambardella *et al.*, Nature (London) **416**, 301 (2002).
[6] O. Pietzsch, A. Kubetzka, M. Bode, and R. Wiesendanger, Phys. Rev. Lett. **84**, 5212 (2000).
[7] M. Albrecht, T. Furubayashi, M. Przybylski, J. Korecki, and U. Gradmann, J. Magn. Magn. Mater. **113**, 207 (1992).
[8] M. Bode *et al.*, Phys. Rev. Lett. **89**, 237205 (2002).
[9] S. Dhesi *et al.*, Phys. Rev. Lett. **87**, 067201 (2001).
[10] Y. L. Iunin *et al.*, Phys. Rev. Lett. **98**, 117204 (2007).
[11] G. Rodary *et al.*, Phys. Rev. B **75**, 184415 (2007).
[12] R. K. Kawakami *et al.*, Phys. Rev. B **58**, R5924 (1998).
[13] R. K. Kawakami *et al.*, Phys. Rev. Lett. **77**, 2570 (1996).
[14] R. Sellman *et al.*, Surf. Sci. **495**, 185 (2001).
[15] H. F. Ding *et al.*, Phys. Rev. B **63**, 134425 (2001).
[16] C. A. F. Vaz, S. J. Steinmuller, and J. A. C. Bland, Phys. Rev. B **75**, 132402 (2007).
[17] J. Ferré *et al.*, Phys. Rev. B **55**, 15 092 (1997).